Bull. Mater. Sci. (2021) 44:97
https://doi.org/10.1007/s12034-021-02372-y

Composition dependence in mechanical properties of zinc-blende compounds associated with the $Cd_xZn_{1-x}S_yTe_{1-y}$ system: a density functional study

SAYANTIKA CHANDA, MANISH DEBBARMA, DEBANKITA GHOSH, BIMAL DEBNATH and SURYA CHATTOPADHYAYA*
Department of Physics, Tripura University, Tripura 799022, India
*Author for correspondence (surya_ju@yahoo.com)

MS received 21 September 2020; accepted 5 November 2020

Abstract. Mechanical characteristics of zinc-blende $Cd_xZn_{1-x}S_yTe_{1-y}$ alloys and their cationic (Cd) and anionic (S) composition dependence ($0.0 \leq x, y \leq 1.0$) have been computed with density functional theory. Elastic stiffness constants and hardness of specimens increase nonlinearly with enhancement in sulphur concentration at any cadmium concentration, whereas each of them has been decreased with increase in cadmium concentration at each fixed sulphur concentration. Each compound is mechanically and dynamically stable, elastically anisotropic, ductile, fairly compressible and plastic in nature. Again, leading role of covalent over ionic and bending over stretching in chemical bonds, central nature of interatomic forces are calculated in case of each specimen. Computed Debye temperature predicts that ZnS is the hardest and CdTe is the softest compared to the other specimens. Calculations of Gruneisen parameters predict that interatomic interactions in each compound show anharmonicity. Thermal conductivity and melting temperature of each compound have also been calculated.

Keywords. $Cd_xZn_{1-x}S_yTe_{1-y}$ alloys; density functional study; PBE–GGA functional; mechanical features; sulphur and cadmium composition dependence.

1. Introduction

In materials science and engineering, simultaneous regulation of concentrations of two elements through doping in quaternary alloys is established to be advantageous over ternary alloys, where regulation of concentration of only one element is possible. It has established the designing of quaternary alloys as a superior method for tuning various properties with enhanced precision than the ternary alloys for broadening the range of specific applications.

It is well known that doping of Cd atom(s) in ZnS and ZnTe crystals constitute cationic ternary $Cd_xZn_{1-x}S$ and $Cd_xZn_{1-x}Te$ alloys, S atom(s) in CdTe and ZnTe crystals constitute anionic ternary CdS_yTe_{1-y}, ZnS_yTe_{1-y} alloys and S atom(s) in $Cd_xZn_{1-x}Te$ ternary crystal constitute $Cd_xZn_{1-x}S_yTe_{1-y}$ quaternary alloys. Therefore, all these binary, ternary and quaternary compounds are the members of $Cd_xZn_{1-x}S_yTe_{1-y}$ family. The present article contains mechanical properties for all the previously mentioned members of $Cd_xZn_{1-x}S_yTe_{1-y}$ family in order to get an idea about their direct/indirect linkage with several fundamental properties. It is to be noted that the calculated mechanical properties of almost all the previously mentioned ternary as well as any of the quaternary alloys have never been reported earlier.

A large number of optoelectronic devices have been fabricated with group IIB–VIA diatomic wide-direct-band-gap (Γ–Γ) cadmium sulphide (CdS), cadmium telluride (CdTe), zinc sulphide (ZnS) and zinc telluride (ZnTe), which are crystallized in zinc-blende (B3) structure under ambient situations [1–13]. The lattice constants and elastic properties of these zinc-blende diatomic chalcogenides have been investigated experimentally [14–25]. Moreover, several first-principle calculations have been carried out in order to calculate lattice constants [26–29] as well as mechanical properties [30–46] of these zinc-blende diatomic compounds.

No experimental investigations has been performed regarding mechanical properties of CdS_yTe_{1-y} and ZnS_yTe_{1-y} anionic ternary alloys, $Cd_xZn_{1-x}S$ and $Cd_xZn_{1-x}Te$ cationic ternary alloys and $Cd_xZn_{1-x}S_yTe_{1-y}$ quaternary alloys. Only a couple of first-principle

Electronic Supplementary Information: The online version contains supplementary material available at https://doi.org/10.1007/s12034-021-02372-y.

Published online: 16 April 2021

calculations have been carried out on few elastic features of $Cd_xZn_{1-x}Te$ ternary alloys [47,48]. Therefore, it is necessary to calculate accurately the elastic properties of the remaining CdS_yTe_{1-y}, ZnS_yTe_{1-y} and $Cd_xZn_{1-x}S$ ternary as well as $Cd_xZn_{1-x}S_yTe_{1-y}$ quaternary alloys to fulfil their requirements in different technological applications.

In this article, we have presented for the first time the computed elastic properties of the zinc-blende $Cd_xZn_{1-x}S_yTe_{1-y}$ quaternary alloys and their intermediate CdS_yTe_{1-y}, ZnS_yTe_{1-y} and $Cd_xZn_{1-x}S$ ternary compounds ($0.0 \leq x, y \leq 1.0$) in an elaborate manner. Moreover, elastic properties of the another set of intermediate ternary compounds under $Cd_xZn_{1-x}Te$ system and the basic constituent binaries CdS, ZnS, CdTe and ZnTe have also been calculated and presented in this article. Considering the complete range of composition of cadmium (cationic composition) x and that of sulphur (anionic composition) y ($0.0 \leq x, y \leq 1.0$) as well as segregating the entire rectangular quaternary $Cd_xZn_{1-x}S_yTe_{1-y}$ system in two binary-ternary and three ternary–quaternary sub-systems, the composition dependence of calculated mechanical properties have been studied.

2. Method of calculations

Our computations have been executed with the WIEN2K code [49], a realization of density functional theory (DFT) [50,51] based FP-LAPW method [52] in practice. We have used the cubic2-elastic code [53], worked in collaboration with WIEN2K, to compute the elastic properties of each cubic crystal. The required exchange-correlation (XC) potentials have been computed with the Perdew–Burke–Ernzerhof generalized gradiant approximation (PBE–GGA) scheme [54]. The XCrySDen [55] graphic code has been utilized for visualization purpose.

The FP-LAPW method is based on the muffin-tin structure, where muffin-tin spheres, subject to fulfillment of non-overlapping criteria, include atoms. In order to expand the Kohn–Sham wavefunctions, spherical harmonics are used with maximum angular momentum $l_{max} = 10$. In contrary, same has been performed in the regions between muffin-tin spheres with plane wave basis with largest K-vector $K_{max} = 8.0/R_{MT}$ and Fourier expansion parameter $G_{max} = 16\text{Ry}^{1/2}$. Both the non-overlapping criteria and non-leakage of core charge criteria have been fulfilled by selecting minimum muffin-tin spheres radii (R_{MT}) enclosing cadmium, zinc, sulphur and tellurium atoms as 2.5, 2.4, 2.2 and 2.5 a.u., respectively. Integrations over the first Brillouin zone have been performed with 1500 k-points. To attain total energy convergence through self-consistent-field (SCF) method, an energy 10^{-5} Ry is incorporated as the threshold.

3. Results and discussions

3.1 *Lattice constant*

For simulated unit cell of any specimen under consideration, SCF calculations with respect to cell parameters and atomic positions have been carried out in order to calculate its minimum energy. In the subsequent stage, lattice constant (a_0) of a cubic crystal is evaluated by fitting the parabolic total energy *vs.* volume curve with equation of state of Murnaghan [56]. In table 1, the calculated a_0 for each cubic unit cell has been presented. Comparison of calculated a_0 for ternary and quaternary specimens are not possible as a result of absence of any corresponding experimentally observed or previously calculated data in literature. In contrary, computed a_0 for binary compound fairly agree with corresponding experimental lattice constant of ZnS, ZnTe, CdS and CdTe [23] as well as some previously calculated data for ZnS, ZnTe [26,27,33,35,36], CdS and CdTe [26,29,39]. Nonlinear decrease in computed a_0 with growing concentration of sulphur (y) at any concentration of cadmium (x) is shown in figure 1a. In contrary, figure 1a also shows that calculated a_0 enhances with the growth of x at any fixed y.

3.2 *Elastic features*

3.2a *Elastic constants, mechanical and dynamical stabilities.* Reduction in amount of symmetries in a crystal demands larger number of deformations and it results in an increase in number of independent elastic constants [57]. Any zinc-blend crystal involves only three non-zero independent elastic stiffness constants C_{11}, C_{12} and C_{44} due to high symmetry [58]. In any cubic crystal, first one is linked to longitudinal deformation, while the remaining two are linked to shearing deformation. Calculations of C_{11}, C_{12} and C_{44} for each specimen have been reported in table 1. Nonlinear increase in calculated C_{11}, C_{12} and C_{44} with increase in composition of sulphur (y) at any composition of cadmium (x) have been shown in figure 1b–d, respectively, where decrease in calculated C_{11}, C_{12} and C_{44} with increase in x at any value of y have also been observed.

Any experimentally measured C_{11}, C_{12} and C_{44} for CdS as well as experimental and previous theoretical elastic constants for the considered ternary and quaternary alloys are unavailable. In contrast, our calculated elastic constants for binary compounds show excellent agreement with respective experimental data for CdTe [14,15,25], ZnS and ZnTe [15] and some of their previously calculated data, reported in table 1. Again, the trend $C_{11}>C_{12}>C_{44}$ for each of the specimens, observed in table 1, have been authenticated with the previously mentioned experimental or previous theoretical studies in the case of binary compounds only.

Table 1. Calculated a_0, C_{11}, C_{12}, C_{44} and C' for the zinc-blende specimens.

x	y	Specimen	a_0 (Å)	C_{11} (GPa)	C_{12} (GPa)	C_{44} (GPa)	C'(GPa)
0.0	0.0	ZnTe	6.109	71.59	40.21	31.74	15.69
			6.089[a*]	71.3[b*]	40.7[b*]	31.2[b*]	
			6.10[a], 6.00[b]	71.1±0.03[c*]	40.7±0.04[c*]	31.3±0.02[c*]	
			6.078[d], 6.020[e]	82.0[b], 62.95[d]	42.0[b], 40.62[d]	55.0[b], 43.16[d]	
	0.25	$ZnS_{0.25}Te_{0.75}$	6.054	82.05	47.40	36.55	17.33
	0.50	$ZnS_{0.50}Te_{0.50}$	5.863	90.94	54.66	40.80	18.14
	0.75	$ZnS_{0.75}Te_{0.25}$	5.672	98.60	60.95	44.37	18.83
	1.0	ZnS	5.416	103.2	66.20	46.77	18.50
			5.412[a*]	104.6[b*]	65.3[b*]	46.13[b*]	
			5.38[a], 5.342[b], 5.335[c], 5.383[d], 5.302[e]	118.0[b], 123.7[c], 110.15[d]	72.0[b], 62.1[c], 63.71[d]	75.0[b], 59.7[c], 60.41[d]	
0.25	0.0	$Cd_{0.25}Zn_{0.75}Te$	6.240	67.64	38.46	28.98	14.59
	0.25	$Cd_{0.25}Zn_{0.75}S_{0.25}Te_{0.75}$	6.175	78.10	45.65	33.79	16.23
	0.50	$Cd_{0.25}Zn_{0.75}S_{0.50}Te_{0.50}$	6.005	86.99	52.91	38.04	17.04
	0.75	$Cd_{0.25}Zn_{0.75}S_{0.75}Te_{0.25}$	5.813	94.65	59.20	41.61	17.73
	1.0	$Cd_{0.25}Zn_{0.75}S$	5.504	99.23	64.45	43.81	17.39
0.50	0.0	$Cd_{0.50}Zn_{0.50}$ Te	6.352	63.69	36.71	26.43	13.49
	0.25	$Cd_{0.50}Zn_{0.50}S_{0.25}Te_{0.75}$	6.289	74.15	43.90	31.03	15.13
	0.50	$Cd_{0.50}Zn_{0.50}S_{0.50}Te_{0.50}$	6.124	83.04	51.16	35.28	15.94
	0.75	$Cd_{0.50}Zn_{0.50}S_{0.75}Te_{0.25}$	5.933	90.70	57.45	38.85	16.63
	1.0	$Cd_{0.50}Zn_{0.50}$ S	5.632	95.28	62.50	41.05	16.39
0.75	0.0	$Cd_{0.75}Zn_{0.25}Te$	6.422	59.64	34.96	23.86	12.34
	0.25	$Cd_{0.75}Zn_{0.25}S_{0.25}Te_{0.75}$	6.393	70.20	42.15	28.24	14.03
	0.50	$Cd_{0.75}Zn_{0.25}S_{0.50}Te_{0.50}$	6.229	79.09	49.41	32.32	14.84
	0.75	$Cd_{0.75}Zn_{0.25}S_{0.75}Te_{0.25}$	6.04	86.75	55.70	35.89	15.53
	1.0	$Cd_{0.75}Zn_{0.25}S$	5.751	91.40	60.35	38.29	15.53
1.0	0.0	CdTe	6.508	55.99	33.31	21.65	11.34
			6.48[a*], 6.447[e], 6.64[f], 6.496[p]	53.51[b*,d*], 53.6[e*], 59.0[f], 58.9[g],	36.81[b*,d*], 37.0[e*], 41.8[f], 40.4[g], 39.3[h],	19.94[b*,d*] 20.1[e*]	8.35[f*]
				68.1[h], 59.3[i], 53.2[k], 50.3[l], 53.2[m], 56.75[n]	34.1[i], 23.2[k], 37.69[l], 36.0[m], 40.73[n]	22.3[f], 24.2[g], 22.1[h], 20.1[i], 13.01[k], 12.13[l] 31.8[m], 20.47[n]	11.2[o]
	0.25	$CdS_{0.25}Te_{0.75}$	6.473	66.15	40.40	25.69	12.88
	0.50	$CdS_{0.50}Te_{0.50}$	6.307	75.14	47.66	29.46	13.74
	0.75	$CdS_{0.75}Te_{0.25}$	6.124	82.80	53.85	32.73	14.48
	1.0	CdS	5.831	88.18	58.40	35.03	14.89
			5.82[a*], 5.804[e], 5.94[f], 5.838[p]	67.2[f], 97.8[h], 92.3[i], 89.38[j], 67.6[k]	55.7[f], 59.7[h], 51.2[i], 53.52[j], 46.3[k]	29.3[f], 30.6[h], 26.3[i], 39.11[j], 29.5[k]	7.07[o]

Experimental data: [a*]Ref. [23], [b*]Ref. [15], [c*]Ref. [16], [d*]Ref. [14], [e*]Ref. [25], [f*]Ref. [24].
Previous theoretical data: [a]Ref. [27], [b]Ref. [33], [c]Ref. [35], [d]Ref. [36], [e]Ref. [26], [f]Ref. [39], [g]Ref. [37], [h]Ref. [40], [i]Ref. [41], [j]Ref. [42], [k]Ref. [45], [l]Ref. [43], [m]Ref. [38], [n]Ref. [46], [o]Ref. [44], [p]Ref. [29].

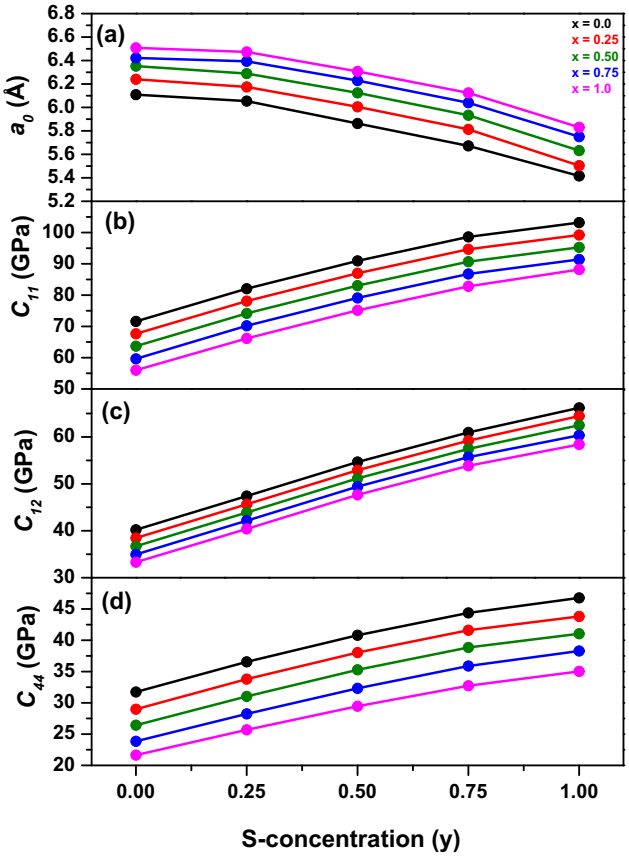

Figure 1. Sulphur composition (y) dependence curves for computed (**a**) a_0, (**b**) C_{11}, (**c**) C_{12} and (**d**) C_{44}.

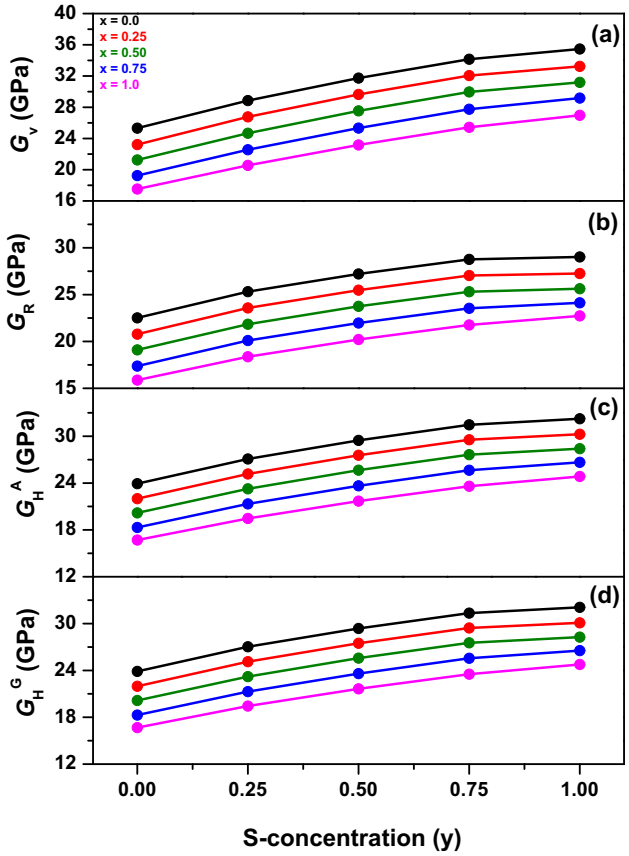

Figure 2. Sulphur composition (y) dependence curves for computed (**a**) G_V, (**b**) G_R, (**c**) G_H^A and (**d**) G_H^G.

In table 1, fulfillment of Born's constraints $C_{11} - C_{12} > 0$; $C_{11} + 2C_{12} > 0$; $C_{11} > 0$; $C_{44} > 0$ imply mechanical stability [59] and positive sign of calculated shear constant $C^{/} = (C_{11} - C_{12})/2$ imply dynamical stability [53] of each cubic binary, ternary and quaternary specimen. Calculated $C^{/}$ for only CdTe is marginally larger than respective experimental data [24], while it agrees excellently well with a previously calculated data [44]. On the other hand, we have observed substantial overestimation of our calculated $C^{/}$ for CdS with respect to the corresponding earlier calculated one [44].

3.2b *Elastic modulus and associated parameters.* Shear modulus of a solid is the resistance of a material to shearing deformation. Its upper and lower boundary of effective shear modulus has been indicated with Voigt shear modulus (G_V) [60] and Reuss shear modulus (G_R) [61], respectively. They have been expressed with C_{11}, C_{12} and C_{44} of a cubic specimen [53]. Hill's shear modulus (G_H) [62] expresses the intermediate conditions for a cubic crystal through either $G_H^A = (G_V + G_R)/2$ or $G_H^G = \sqrt{G_V G_R}$ [63].

Hashin and Shtrikman [64] have proposed alternative expressions for calculating the upper bound (G_U) and lower bound (G_L) of shear modulus in terms of C_{11}, C_{12} and C_{44} of a cubic specimen. The average $G_{HS} = (G_U + G_L)/2$ of shear modulus G_U and G_L, known as Hashin–Shtrikman shear modulus, has expressed the intermediate conditions as per new proposal [64].

In supplementary table ST1, we have presented the calculated G_V, G_R, G_H^A, G_H^G, G_U, G_L and G_{HS}. We have observed insubstantial difference between G_H^A and G_H^G as well as G_U and G_L in case of each of the specimens. From figure 2a–d, we have observed that each of the calculated G_V, G_R, G_H^A and G_H^G, respectively, increases with increase in composition of sulphur (y) at any composition of cadmium (x), while the same has been observed for each of the calculated G_L, G_U and G_{HS} from figure 3a–c, respectively. We have also observed decrease in G_V, G_R, G_H^A and G_H^G in figure 2a–d, respectively, and G_L, G_U and G_{HS} in figure 3a–c, respectively, with increase in x at each fixed y. Calculated G_V, G_R, G_H^G, G_U, G_L and G_{HS} cannot be compared as a result of lacking of experimentally investigated or earlier calculated data in any published articles. In contrary, computed G_H^A for both CdS and CdTe are larger by fair amount compared to the experimental data for CdS [25] and CdTe [21] as well as some of their corresponding previous theoretical data [31,37,39,41].

The bulk modulus (B_0) of a solid, reciprocal to its compressibility, is the measure of stiffness under uniform compression over its surface, while Young's modulus (Y)

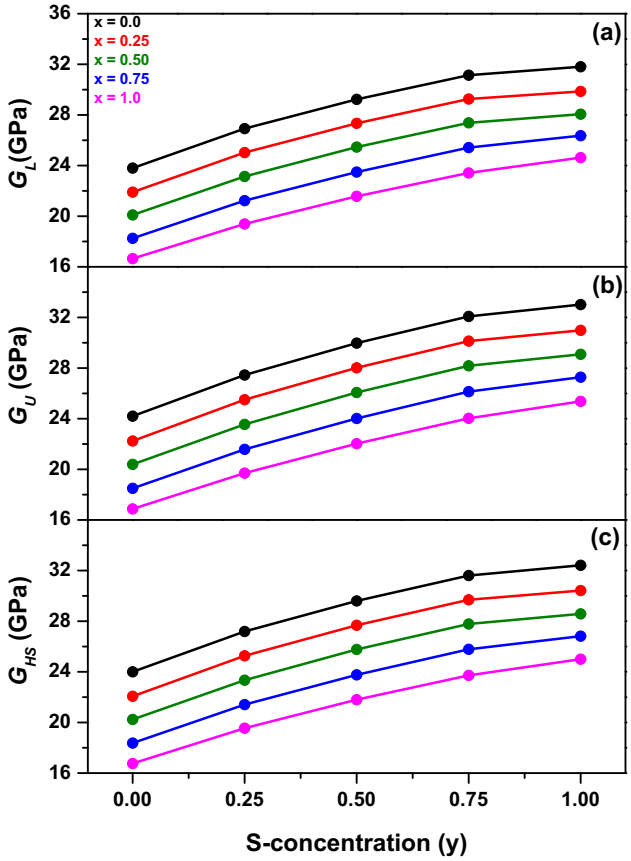

Figure 3. Sulphur composition (y) dependence curves for computed (**a**) G_L, (**b**) G_U and (**c**) G_{HS}.

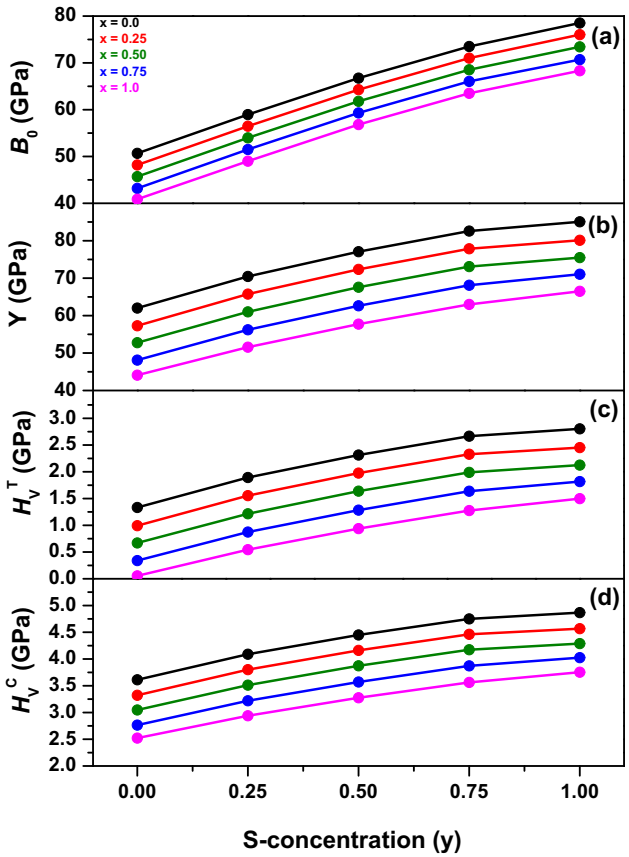

Figure 4. Sulphur composition (y) dependence curves for computed (**a**) B_0, (**b**) Y, (**c**) H_V^T and (**d**) H_V^C.

measures its stiffness under uniaxial deformation. Enhancement in B_0 and Y correspond to improvement in hardness of a solid. The B_0 for a cubic lattice can be computed in terms of its C_{11} and C_{12}, whereas Y can be computed in terms of its B_0 and G_H^A [53].

The Vicker's hardness (H_V) has also been used to calculate the hardness of a solid, which can again be expressed with two different empirical relationships in terms of its Hill's shear modulus (G_H^A). The proposed empirical relation of Teter [65] has been expressed as $H_V^T = 0.1769G_H^A - 2.899$, while another relation $H_V^C = 0.151G_H^A$ has been proposed by Chen and co-workers [66].

In supplementary table ST2, the calculated B_0, Y, H_V^T and H_V^C for each specimen have been presented. The mechanical stability of each compound is once again ensured and subject to fulfillment of the condition $C_{12} < B_0 < C_{11}$. Experimentally investigated Y and both experimentally investigated as well as earlier calculated H_V^T and H_V^C for any specimen is unavailable. Computed B_0 in case of ZnS, ZnTe, CdS and CdTe fairly agree with corresponding experimental [23] and some of the previously calculated [27–29,31,37,39] data. Computed Y in case of CdS and CdTe are showing fair closeness to the earlier theoretical Y for CdS [40] and CdTe [37]. From figure 4a–d, we have observed that each of the calculated B_0, Y, H_V^T and H_V^C, respectively, nonlinearly enhances with growing concentration of sulphur (y) at any concentration of cadmium (x). Decrease in each of the calculated B_0, Y, H_V^T and H_V^C with increasing x at each fixed y is also observed from figure 4a–d, respectively. According to calculations of B_0, Y, H_V^T and H_V^C, the ZnS and CdTe show maximum and minimum hardness, respectively.

In case of any material, the B_0/C_{44} is the indicator of its plasticity [67]. Calculated B_0/C_{44} for each specimen under consideration has been presented in supplementary table ST2. For all the specimens, calculated $B_0/C_{44}>1.5$ indicates their fair plasticity. Experimentally investigated or earlier calculated B_0/C_{44} in case the specimens are unavailable. For any material, ductility or brittleness are generally scrutinized with its calculated Pugh's ratio B_0/G_H^A [68] as well as Cauchy's pressure $C^{//} = C_{12} - C_{44}$ [67]. The $B_0/G_H^A > 1.75$ and positive $C^{//}$ stand for ductility, while $B_0/G_H^A < 1.75$ and negative $C^{//}$ stand for brittleness of a material. Clearly, ductile nature of all the specimens have been confirmed with calculated $B_0/G_H^A > 2.0$ and positive $C^{//}$, presented in supplementary table ST2. Available experimental B_0/G_H^A for only CdTe [14] as well as

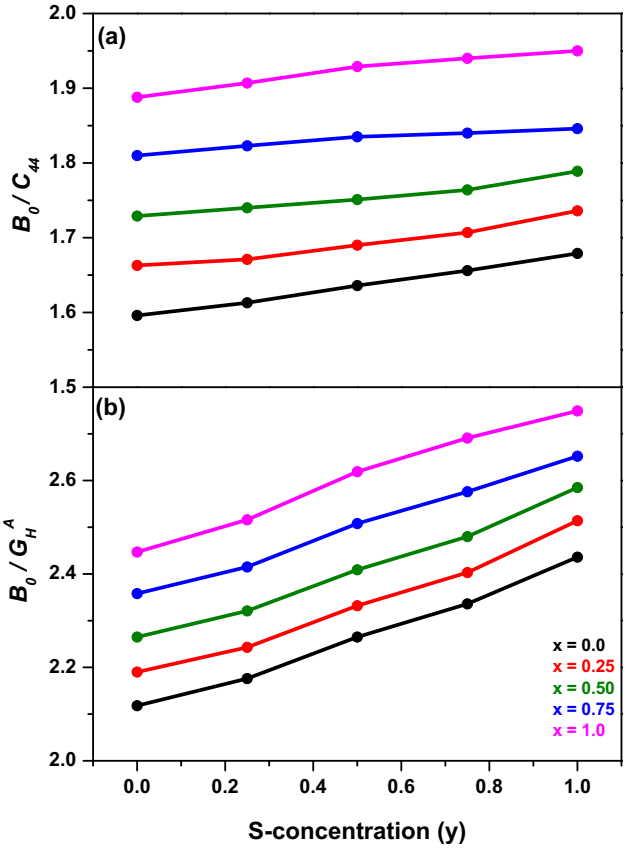

Figure 5. Sulphur composition (y) dependence curves for computed (**a**) B_0/C_{44} and (**b**) B_0/G_H^A.

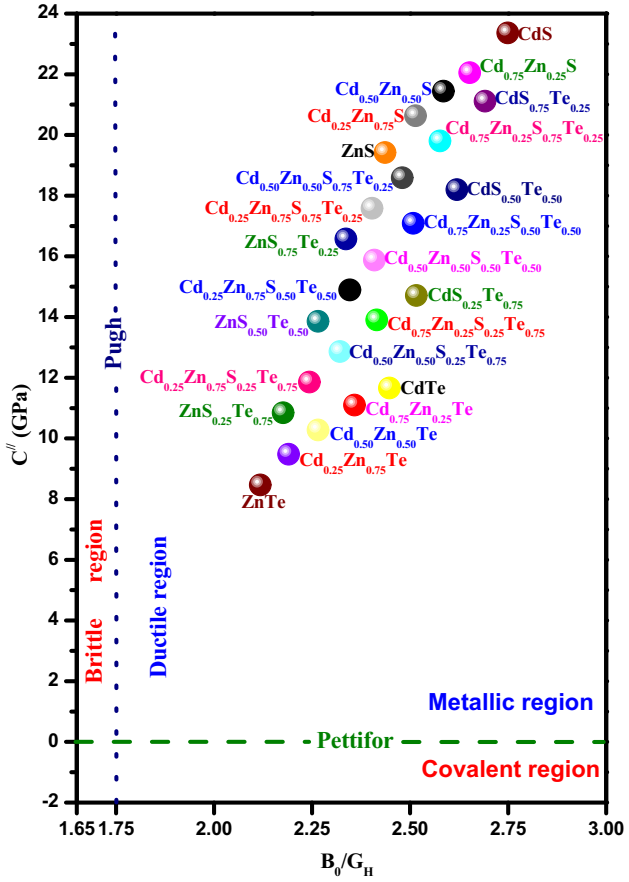

Figure 6. Correlation between Cauchy pressure $C^{//}$ and Pugh's ratio B_0/G_H^A for ductility.

previously calculated data for both CdS [39] and CdTe [37,39] are fairly higher than our respective calculated data. From figure 5a and b, we have observed that each of the calculated B_0/C_{44} and B_0/G_H^A, respectively, enhances nonlinearly with growing composition of sulphur (y) at any composition of cadmium (x) as well as with increasing x at each fixed y. The correlation between $C^{//}$ and B_0/G_H^A of all the compounds, presented in figure 6, clearly indicates the existence of each of the concerned specimens within ductile regime.

The Poisson's ratio σ ($-1 \leq \sigma \leq 0.5$) indicates manifold features of a material. For any material, affinity towards total incompressibility is indicated with $\sigma \rightarrow 0.5$, central nature of bonding force with $0.25 < \sigma < 0.50$, better plasticity with $\sigma \rightarrow 0.5$, poor plasticity with $\sigma \rightarrow -1.0$, brittleness with $\sigma < 0.26$ and ductility with $\sigma > 0.26$ [69]. The σ of any material can be expressed with B_0 and G_H^A [53].

Kleinman parameter ξ ($0 \leq \xi \leq 1$) [70] indicates of relative locations of sublattices of anions and cations inside a crystal under strain distortions at conserved volume. The $\xi = 0$ stands for minimum bond bending, while $\xi = 1$ indicates minimum bond stretching. Kleinman parameter (ξ) in case of a zinc-blende lattice can be computed with its C_{11} and C_{12} [53].

For each specimen, computed σ and ξ are reported in supplementary table ST3. Computed σ for all the compounds, ranging between 0.29 and 0.34, shows their considerable compressibility, ductility, plasticity and central nature of interatomic bonding force. On the other hand, calculated ξ for all the specimens in the range 0.67–0.77 convey considerably governing bending over stretching in chemical bonds. Figure 7a and b displays nonlinear increase in calculated σ and ξ, respectively, with enhancing composition of sulphur (y) at any composition of cadmium (x) as well as with increasing x at each fixed y. In case of any specimen under consideration, experimental σ and ξ is unavailable to compare our calculated data. In contrary, calculated σ in case of CdS and CdTe show fairly closeness to the corresponding earlier calculated σ [37,39,40], while their computed ξ are underestimated by a small amount with respect to the corresponding earlier calculated ξ [39].

3.2c *Isotropic/anisotropic characters of specimens.* The probability of variation of nature of bonding in different directions and hence the probability of occurrence of microscopic cracks in a crystal can be examined by estimating its elastic anisotropy, generally in terms of

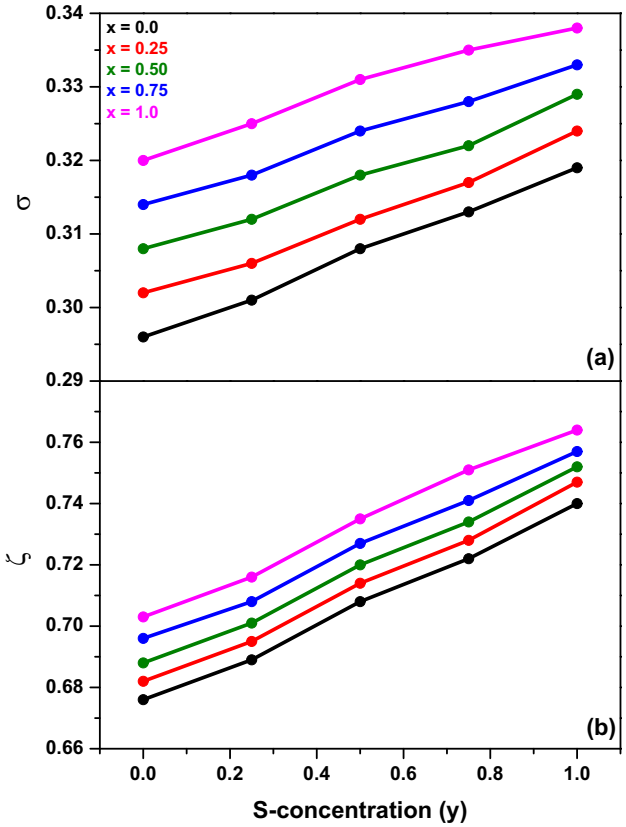

Figure 7. Sulphur composition (y) dependence curves for computed (**a**) σ and (**b**) ζ.

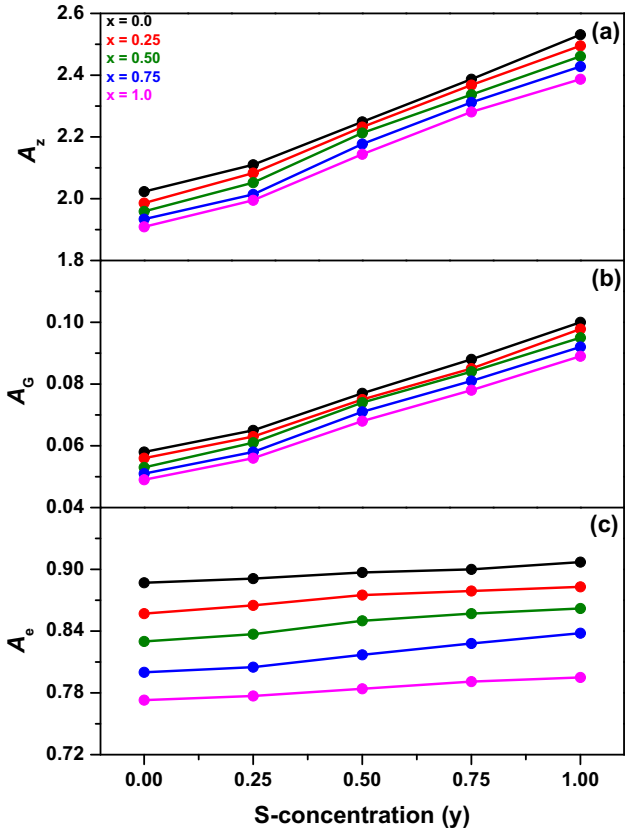

Figure 8. Sulphur composition (y) dependence curves for computed (**a**) A_z, (**b**) A_G and (**c**) A_e.

Zener anisotropy (A_z). For any cubic crystal, A_z has been expressed with C_{11}, C_{12} and C_{44} [53]. Chung and Buessem proposed a relation in terms of G_V and G_R to compute percentage of elastic anisotropy (A_G) in a crystal [71]. Moreover, computation of anisotropy in elastic wave velocity (A_e) is considered to be an alternative way of investigating elastic anisotropy in a cubic crystal [72]. The A_z, A_G and A_e can be expressed as

$$A_z = \frac{2C_{44}}{C_{11} - C_{12}} \tag{1}$$

$$A_G = \frac{G_V - G_R}{G_V + G_R} \tag{2}$$

$$A_e = \frac{2C_{44} + C_{12}}{C_{11}} - 1 \tag{3}$$

The elastic isotropy is indicated with $A_z = 1$. On the other hand, $A_z > 1$ and $A_z < 1$ are the signatures of elastically anisotropic nature with highest stiffness in the direction of $\langle 111 \rangle$ diagonal and in the direction of $\langle 100 \rangle$ axis of the cube, respectively [53]. In any crystal, $A_G = 0$ and $A_G = 1$ stand for 100% isotropy and anisotropy, respectively. Clearly, $A_e = 0$ and $A_e \neq 0$ are the signatures of elastic isotropy and anisotropy, respectively.

Computed A_z, A_G and A_e for the specimens have been presented in supplementary table ST3. Elastic anisotropy for all the specimens along with highest rigidity along $\langle 111 \rangle$ diagonal of the cube is indicated with computed A_z in the range 1.90–2.54. Moreover, elastically anisotropic nature of all the specimens are indicated again with their calculated A_G and A_e in the ranges 0.049–0.100 and 0.773–0.907, respectively.

From figure 8a–c, we have observed that each of the calculated A_z, A_G and A_e, respectively, enhances nonlinearly with growing composition of sulphur (y) at any composition of cadmium (x). Figure 8a–c also convey that each of the calculated A_z, A_G and A_e, respectively, reduces with increasing x at each fixed y. For any specimen, there is no reported experimental A_z as well as experimental or earlier calculated A_G and A_e, while computed A_z in case of each of the CdS and CdTe is found to be in between two earlier calculated A_z [39,40].

Elastic isotropy/anisotropy in a crystal is also investigated from calculations of its Lame's constants λ and μ. The elastic isotropy in a cubic crystal is observed subject to the fulfilment of the constraints $\lambda = C_{12}$, and $\mu = C^{/}$=C_{44} [53]. Each of the Lame's constants of a crystal is expressible in terms of its Y and σ [53].

Supplementary table ST3 contains computed λ and μ of all the specimens. Elastic anisotropy in each of the cubic

specimens is again confirmed through the observed violation of the previously mentioned constraints of isotropy. For any specimen, experimentally investigated or earlier calculated Lame's constants are unavailable in order to verify our computed data.

3.2d *Ionicity, covalency and bonding characteristics.* In any zinc-blende crystal, Potter [73] has proposed that the elastic constant ratio $C_{11}/C_{12} = 1.0$, $C_{11}/C_{12} = 2.0$ and $1.0 < C_{11}/C_{12} < 2.0$ signify perfectly ionic, perfectly covalent and mixture of both, respectively. The following relation between C_{11}/C_{12} and ionic charge Z/Z_0 was again proposed by Potter [73]

$$\frac{Z}{Z_0} = \left[\frac{1}{1.65}\left(\frac{C_{11}}{C_{12}} - 2.65\right)\right]^2 \tag{4}$$

Clearly, Z/Z_0 increases as C_{11}/C_{12} decreases and vice versa. It means that ionic charge equals to unity is indicating completely ionic, while its value 0.155 is indicating completely covalent and any intermediate value is indicating mixture of both types in any crystal.

Supplementary table ST4 contains computed C_{11}/C_{12} and Z/Z_0 for each zinc-blende compound under consideration. Since computed C_{11}/C_{12} and Z/Z_0 are in the range 1.503–1.780 and 0.278–0.484, respectively, mixed type of bonding with leading role of covalent exists in each crystal. From figure 9a and b, we have observed that computed C_{11}/C_{12} reduces, while computed Z/Z_0 enhances nonlinearly, respectively, with growing composition of sulphur (y) at any composition of cadmium (x) as well as with increasing x at each fixed y. For comparison, we do not get any experimentally investigated or earlier calculated C_{11}/C_{12} and Z/Z_0 for any compound.

Based on bond-orbital model, covalency α_C and Philip ionicity f_i of a zinc-blende crystal is calculated through ratio of elastic stiffness constants C_{11}/C_{12} and α_C, respectively, in the following way [74]

$$\alpha_c = \sqrt{\frac{2(C_{11} - C_{12})}{C_{11} + 2C_{12}}} \tag{5}$$

$$f_i = 1 - \alpha_C^2 \tag{6}$$

In supplementary table ST4, computed α_C and f_i for each zinc-blende specimen have been presented. From figure 10a and b, we have observed that computed α_C reduces, but f_i enhances nonlinearly, respectively, with growing composition of sulphur (y) at any composition of cadmium (x) as well as with increasing x at each fixed y. Experimentally investigated or previously calculated α_C for any specimen is

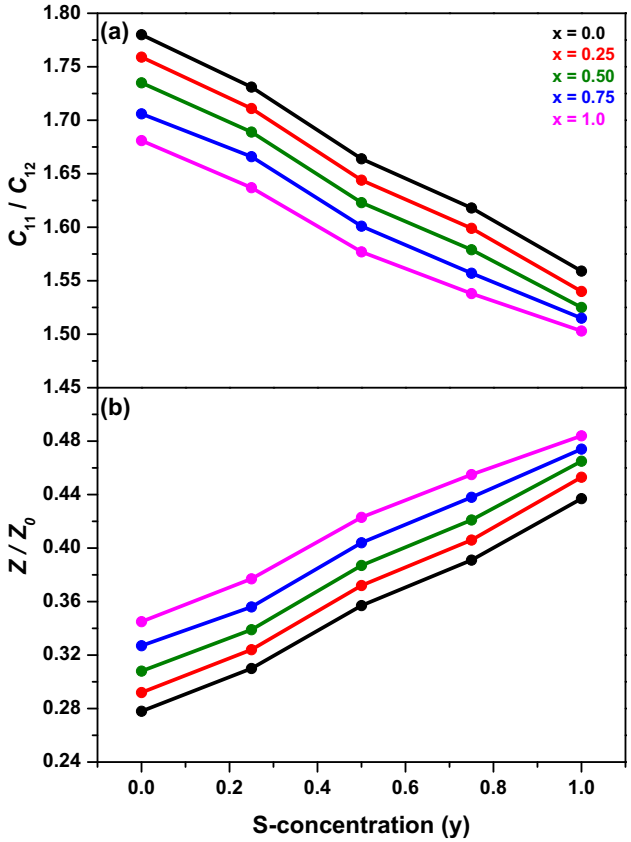

Figure 9. Sulphur composition (y) dependence curves for computed (**a**) C_{11}/C_{12} and (**b**) Z/Z_0.

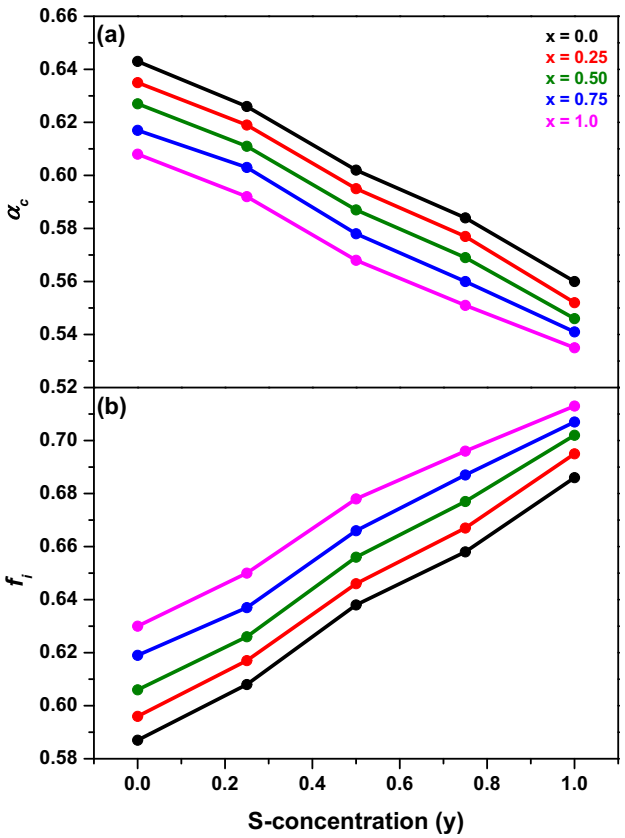

Figure 10. Sulphur composition (y) dependence curves for computed (**a**) α_c and (**b**) f_i.

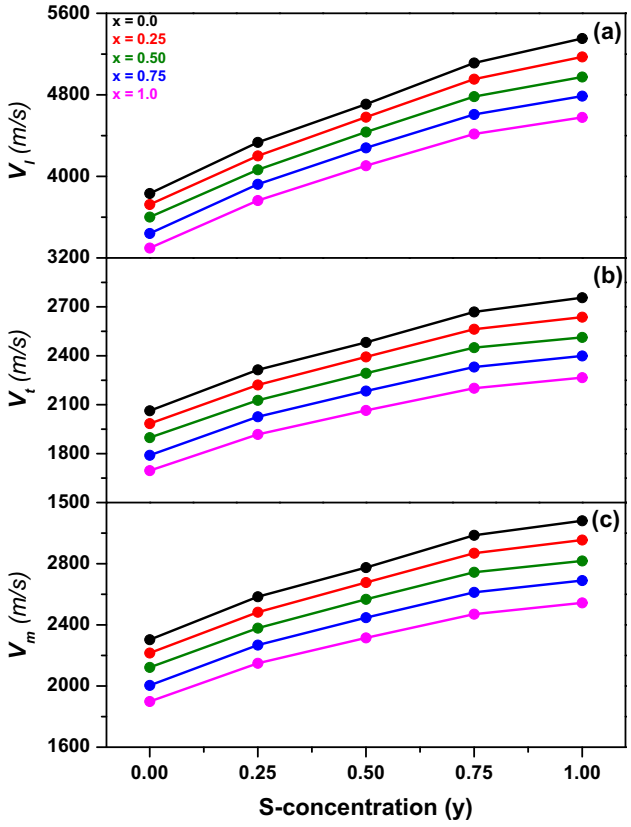

Figure 11. Sulphur composition (y) dependence curves for computed (**a**) v_l, (**b**) v_t and (**c**) v_m.

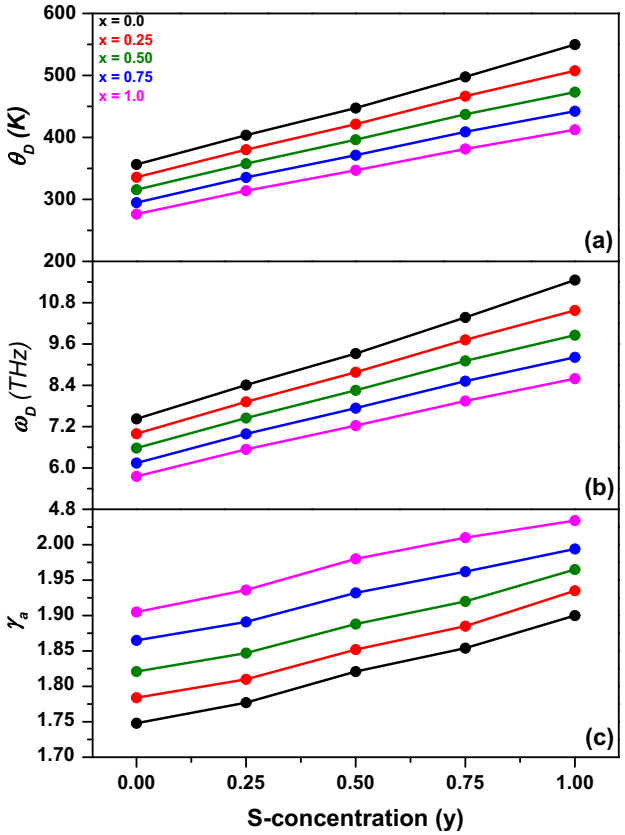

Figure 12. Sulphur composition (y) dependence curves for computed (**a**) θ_D, (**b**) ω_D and (**c**) γ_a.

not available. In contrary, computed f_i for CdS and CdTe have been observed to be fairly close to the corresponding experimentally measured f_i [20].

3.2e *Acoustic velocities, Debye temperature, Debye frequency and Grüneisen parameter.* Distinction of classical and quantum characters of phonons in a solid is achieved through Debye temperature (θ_D) [57]. A solid exposes its quantum mechanical nature at any temperature below θ_D. The acoustical vibrations are solely considered as the origin of vibrational excitations at $T<\theta_D$. Therefore, θ_D of a solid is calculated in terms of mean acoustic velocity (v_m) [75]. The v_m for a solid is calculated from its longitudinal (v_l) and transverse (v_t) acoustic velocities [75]. The v_l for a solid is connected to its G_H^A and B_0, while as v_t to its G_H^A and material density ρ [72].

Supplementary table ST4 includes computed v_l, v_t and v_m for all the specimens. From figure 11a–c, we have observed that each of the computed v_l, v_t and v_m, respectively, enhances nonlinearly with growing composition of sulphur (y) at any composition of cadmium (x), while each of them is observed to be decreased with increasing x at each fixed y. Any experimental or previous theoretical acoustic velocities v_l, v_t and v_m for any specimen are unavailable for comparison.

Debye frequency (ω_D) of a solid, the frequency of maximum atomic vibrations in a solid during thermal transportation, is expressible in terms of its Debye temperature (θ_D) [76]. Supplementary table ST5 includes computed θ_D and ω_D in case of all the specimens. From figure 12a and b, we have observed that each of the computed θ_D and ω_D, respectively, enhances nonlinearly with growing composition of sulphur (y) at any composition of cadmium (x), while each of them is observed to be reduced with increasing x at any fixed y.

Experimentally investigated θ_D and ω_D for the specimens are unavailable. Computed θ_D for each of the CdS and CdTe is highly overestimated with respect to corresponding previously calculated θ_D [39]. Better stiffness due to stronger interatomic force in a solid is indicated with its larger value of Debye temperature θ_D and vice versa, [77] and it indicated that ZnS and CdTe show most and least stiffness, respectively, compared to the other considered compounds.

The Grüneisen parameter (γ_a) in case of a sloid, the signature of anharmonicity in inter-atomic interactions in the solid, is expressible in terms of its v_l and v_t in the following way [78]

$$\gamma_a = \frac{9(V_l^2 - \frac{4}{3}V_t^2)}{2(V_l^2 + 2V_t^2)} \tag{7}$$

Supplementary table ST5, containing computed γ_a of all the considered cubic compounds, is indicates anharmonic nature of atom–atom interactions in each crystal. From

figure 12c, we have observed that computed γ_a enhances nonlinearly with growing composition of sulphur (y) at any composition of cadmium (x) as well as with increasing x at any fixed y. The calculated γ_a for any specimen cannot be compared as a result of deficiency of their experimental or earlier theoretical γ_a.

3.2f *Thermal conductivity and melting point of the specimens.* By measuring thermal conductivity of a solid, we can acquire a clear idea about its capacity of conducting heat. It is a vital parameter in thermal blockade coating related applications [79,80]. The empirical equation, proposed by Liu and co-workers [81] to compute minimum thermal conductivity ($K_{\min}$) of solid is

$$K_{\min} = k_B v_m \left(\frac{M}{n\rho N_a}\right)^{-\frac{2}{3}} \tag{8}$$

The empirical equation, projected by Fine and co-workers [82], to compute melting temperature (T_m) for a cubic crystal is

$$T_m = [553 + (5.91/GPa)C_{11}] \tag{9}$$

Calculated $K_{\min}$ and T_m of each specimen have been reported in supplementary table ST5. Figure 13a and b have displayed nonlinear increase in calculated $K_{\min}$ and T_m, respectively, with growing composition of sulphur (y) at any fixed composition of cadmium (x), while calculated $K_{\min}$ and T_m have been observed to be decreased with increasing x at each fixed y. The calculated $K_{\min}$ and T_m for any specimen cannot be verified due to lack of their experimental or previously calculated $K_{\min}$ and T_m in literature.

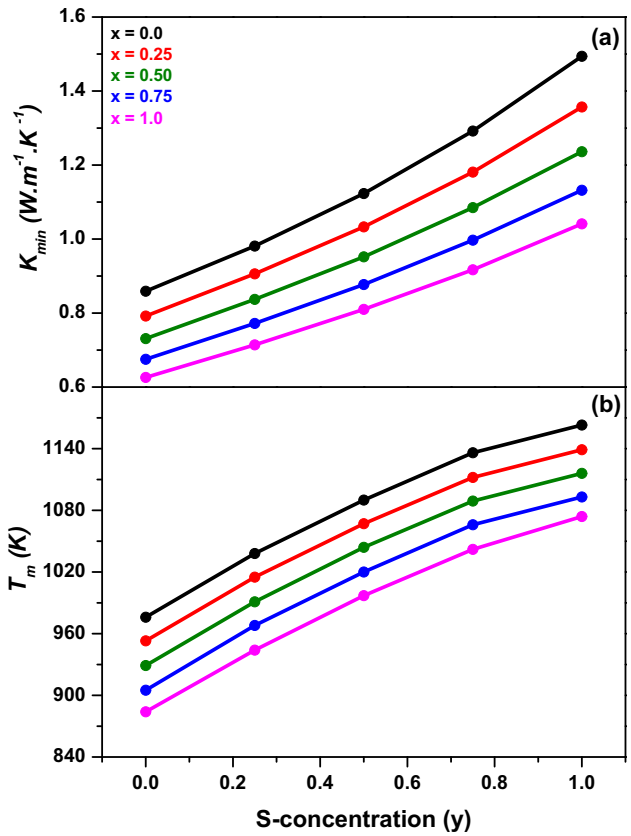

Figure 13. Sulphur composition (y) dependence curves for computed (**a**) $K_{\min}$ and (**b**) T_m.

4. Conclusion

Elastic properties of cubic specimens under $Cd_xZn_{1-x}S_yTe_{1-y}$ quaternary system have been investigated through first-principle calculations. Elastic stiffness constants have shown nonlinear increasing trend with increasing composition of sulphur at any fixed composition of cadmium, while reverse trends are investigated with increasing composition of cadmium at each fixed composition of sulphur in two binary–ternary and three ternary–quaternary systems. Computed elastic stiffness constants have confirmed mechanical stabilities, while calculated shear constants confirm dynamical stabilities of the specimens. Computed bulk, Young's and Shear moduli as well as Vicker's empirical relations, indicating hardness of specimens, are enhanced nonlinearly with enhancing composition of sulphur at any fixed composition of cadmium, while reverse are observed with enhancing composition of cadmium at each fixed composition of sulphur in two binary–ternary and three ternary–quaternary systems. Elastically anisotropic character of each specimen is confirmed from computed Zener anisotropy and Lame's constants. Leading role of bending over stretching in chemical bonds of each specimen is confirmed from calculated Kleinmann parameter. Computed Poisson's ratio, Pugh's ratio and Cauchy pressure confirm ductile nature of each specimen. Fair plasticity in each specimen is confirmed from computed Poisson's ratio and B_0/C_{44}. Blending of covalent and ionic bonding with leading role of covalent in each specimen is confirmed from computed $C_{11}/C_{12}, Z/Z_0, \alpha_C$ and f_i. Maximum stiffness in ZnS and minimum in CdTe compared to other considered specimens are confirmed from computed Debye temperature. Computed Gruneisen parameter indicates anharmonic nature of atom–atom interactions in each specimen. Computed thermal conductivities and melting temperatures for all the specimens indicate that the considered specimens would be suitable in diverse thermal blockade coatings and thermal management system related applications.

Acknowledgements

Ms Sayantika Chanda is thankful to the Department of Science and Technology (DST), Government of India, for providing DST-INSPIRE-JRF [Ref. No DST/INSPIRE/03/2017/002068]. We are also thankful to the University Grants Commission (UGC), Government of India, for

providing financial assistance through UGC-SAP program 2016 [Ref. No F.530/23/DRS-I/2018 (SAP-I)].

References

[1] Nelmes R J and McMahon M I 1998 *Structural transitions in the group IV, III-V, and II-VI semiconductors under pressure* In: T Suski and W Paul (eds) (New York: Academic Press) **54** p 145

[2] Wang J and Isshiki M 2006 *Wide-band-gap ii–vi semiconductors: growth and properties, Springer handbook of electronic and photonic materials* (Berlin: Springer) p 325

[3] Huynh W U, Dittmer J J and Alivisato A P 2002 *Science* **295** 2425

[4] Crossay A, Buecheler S, Kranz L, Perrenoud J, Fella C M, Romanyuk Y E *et al* 2012 *Sol. Energy Mater. Sol. Cells* **101** 283

[5] Okamoto T, Hayashi R, Ogawa Y, Hosono A and Doi M 2015 *Japan J. Appl. Phys.* **54** 04DR01

[6] Ohta T 2001 *J. Opto-Electron. Adv. Mater.* **3** 609

[7] Wagner H P, Wittmann S, Schmitzer H and Stanzl H 1995 *J. Appl. Phys.* **77** 3637

[8] Tamargo M C, Brasil M J S P, Nahory R E, Martin R J, Weaver A L and Gilchrist H L 1991 *Semicond. Sci. Technol.* **6** A8

[9] Fang X, Zhai T, Gautam U K, Li L, Wu L, Bando Y *et al* 2011 *Prog. Mater. Sci.* **56** 175

[10] Hasse M A, Qui J, De Puydt J M and Cheng H 1991 *Appl. Phys. Lett.* **59** 1272

[11] Shieh F, Saunders A E and Korgel B A 2005 *J. Phys. Chem. B* **109** 8538

[12] Peng Z A and Peng X G 2001 *J. Am. Chem. Soc.* **123** 183

[13] Xi L F, Chua K H, Zhao Y Y, Zhang J, Xiong Q H and Lam Y M 2012 *RSC Adv.* **2** 5243

[14] Mcskimin H J and Thomas D G 1962 *J. Appl. Phys.* **33** 56

[15] Berlincourt D, Jafee H and Shlozawa L R 1963 *Phys. Rev.* **129** 1009

[16] Lee B H 1970 *J. Appl. Phys.* **41** 2984

[17] Lee B H 1970 *J. Appl. Phys.* **41** 2988

[18] Gust W H 1982 *J. Appl. Phys.* **53** 4843

[19] Vagelatos N, Wehe D and King J S 1974 *J. Chem. Phys.* **50** 3613

[20] Phillips J C 1970 *Rev. Mod. Phys.* **42** 317

[21] Dunstan D J, Prins A D, Gil B and Faurie J P 1991 *Phys. Rev. B* **44** 4017

[22] Berding M A, Nix W D, Rhiger D R, Sen S and Sher A 2000 *J. Electron. Mater.* **29** 676

[23] Medelung O (ed) 1982 *Landolt Bornstein: numerical data and functional relationship in science and technology* (Berlin: Springer) **17b**

[24] Harrison W A 1980 *Electronic structure and the properties of solids* Freeman, New York

[25] Bass J D 1995 *Mineral physics and crystallography: a handbook of physical constants* T J Ahrens (ed) (USA: American Geophysical Union) p 45

[26] Chen X J, Mintz A, Hu J S, Hua X L, Zinck J and Goddard W A III 1995 *J. Vac. Sci. Technol. B* **13** 1715

[27] Murtaza G, Ullah N, Rauf A, Khenata R, Omran S B, Sajjad M *et al* 2015 *Mater. Sci. Semicond. Process.* **30** 462

[28] Debbarma M, Sarkar U, Debnath B, Ghosh D, Chanda S, Bhattacharjee R *et al* 2018 *J. Alloys Comp.* **748** 446

[29] Debbarma M, Sarkar U, Debnath B, Ghosh D, Chanda S, Bhattacharjee R *et al* 2018 *Appl. Phys.* **18** 698

[30] Martin R M 1970 *Phys. Rev. B* **1** 4005

[31] Kamran S, Chen K and Chen L 2008 *Phys. Rev. B* **77** 094109

[32] Singh R K and Singh S 1987 *Phys. Stat. Sol. B* **140** 407

[33] Khenata R, Bouhemadou A, Sahnoun M, Reshak A H, Baltache H and Rabah M 2006 *Comp. Mater. Sci.* **38** 29

[34] Soykan C, Kart S O and Cagin T 2010 *Arch. Mater. Sci. Eng.* **46** 115

[35] Casali R A and Christensen N E 1998 *Sol. Stat. Commun.* **108** 793

[36] Bilal M, Shafiq M, Ahmad I and Khan I 2014 *J. Semicond.* **35** 0720011

[37] Zeng W, Liu Q J and Liu Z T 2016 *J. Appl. Phys.* **1** 26

[38] Agrawal B K and Agrawal S 1992 *Phys. Rev. B* **45** 8321

[39] Guo L, Zhang S, Feng W, Hu G and Li W 2013 *J. Alloys Compd.* **579** 583

[40] Deligoz E, Colakoglu K and Ciftci Y 2006 *Physica B* **373** 124

[41] Sharma S, Verma A S, Sarkar B K, Bhandari R and Jindal V K 2011 *AIP Conf. Proc.* **1393** 229

[42] Wright K and Gale J D 2004 *Phys. Rev. B* **70** 035211

[43] Kanoun M B, Sekkal W, Aourag H and Merad G 2000 *Phys. Lett. A* **272** 113

[44] Kitamura M, Muramutsu S and Harrison W A 1992 *Phys. Rev. B* **46** 1351

[45] Ouendadji S, Ghemid S, Meradji H and Hassan F El Haj 2011 *Comp. Mater. Sci.* **50** 1460

[46] Rajput B D and Browne D A 1996 *Phys. Rev. B* **53** 9052

[47] Bouarissa N and Atik Y 2008 *Mod. Phys. Lett. B* **22** 1221

[48] Saib S, Benyettou S and Bouarissa N 2015 *Physica E* **68** 184

[49] Blaha P, Schwarz K, Madsen G H, Kbasnicka D and Luitz J 2001 *FP-LAPW+lo Program for Calculating Crystal Properties* K Schwarz (ed)*:* In *WIEN2K-2th Edition* (Vienna: Vienna University of Technology)

[50] Hohenberg P and Kohn W 1964 *Phys. Rev. B* **136** 864

[51] Kohn W and Sham L J 1965 *Phys. Rev.* **140** A1133

[52] Andersen O K 1975 *Phys. Rev. B* **42** 3063

[53] Jamal M, Asadabadi S J, Ahmed I and Aliabad H A R 2014 *Comp. Mater. Sci.* **95** 592

[54] Perdew J P, Burke K and Ernzerhof M 1996 *Phys. Rev. Lett.* **77** 3865

[55] Kokalj A 2003 *Comp. Mat. Sci.* **28** 155

[56] Murnaghan F D 1944 *Proc. Natl. Acad. Sci. USA* **30** 244

[57] Ravindran P, Fast L, Korzhavyi P A and Johansson B 1998 *J. Appl. Phys.* **84** 4891

[58] Mouhat F and Coudert F X 2014 *Phys. Rev. B* **90** 224104

[59] Born M and Huang K 1954 *Dynamics theory of crystal lattices* Oxford University Press, UK

[60] Voigt W 1889 *Ann. Phys.* **38** 573

[61] Reuss A and Angew Z 1929 *Math. Phys.* **9** 49

[62] Hill R 1952 *Proc. Phys. Soc. Lond. A* **65** 349

[63] Ledbetter H M 1973 *J. Appl. Phys.* **44** 1451

[64] Hashin Z and Shtrikman S 1962 *J. Mech. Phys. Solids* **10** 343

[65] Teter D 1998 *MRS Bull.* **23** 22

[66] Chen X Q, Niu H Y, Li D Z and Li Y Y 2011 *Intermetallics* **19** 1275

[67] Pettifor D G 1992 *Mater. Sci. Technol.* **8** 345
[68] Pugh S F 1954 *Philos. Mag.* **45** 823
[69] Frantsevich I N, Voronov F F and Bokuta S A 1983 *Elastic constants and elastic moduli of metals and insulators handbook* Naukova Dumka, Kiev, Kiev
[70] Kleinman L 1962 *Phys. Rev.* **128** 2614
[71] Chung D H and Buessem W R 1968 in: *Anisotropy in Single-crystal refractory compounds: proceedings* Plenum Press, New York
[72] Li S, Li S and Ju X 2017 *J. Alloys Compd.* **695** 2916
[73] Potter R Y 1957 *J. Phys. Chem. Solids* **3** 223
[74] Adachi S 2005 *Properties of group-iv, iii–v and ii–vi semiconductors* Wiley, West Sussex, UK
[75] Anderson O L 1963 *J. Phys. Chem. Sol.* **24** 909
[76] Huang W and Yang L 2015 *Can J. Phys.* **93** 1
[77] Zhang X-D, Hou Z-F, Jiang Z-Y and Hou Y-Q 2011 *Physica B* **406** 2196
[78] Belomestnykh V N 2004 *Tech. Phys. Letts.* **30** 91
[79] Clarke D R and Phillpot S R 2005 *Materialstoday* **8** 22
[80] Clarke D R 2003 *Surf. Coat. Technol.* **67** 163
[81] Liu B, Wang J Y, Li F Z and Zhou Y C 2010 *Acta Mater.* **58** 4369
[82] Fine M E, Brown L D and Marcus H L 1984 *Scr. Metall.* **18** 951